

Enhanced photoresponse of conformal TiO₂/Ag nanorod array-based Schottky photodiodes fabricated via successive glancing angle and atomic layer deposition

Ali Haider, Hilal Cansizoglu, Mehmet Fatih Cansizoglu, Tansel Karabacak, Ali Kemal Okyay, and Necmi Biyikli

Citation: *Journal of Vacuum Science & Technology A: Vacuum, Surfaces, and Films* **33**, 01A110 (2015); doi: 10.1116/1.4898203

View online: <http://dx.doi.org/10.1116/1.4898203>

View Table of Contents: <http://avs.scitation.org/toc/jva/33/1>

Published by the [American Vacuum Society](#)

Articles you may be interested in

[Hydrothermal synthesis of ordered single-crystalline rutile TiO₂ nanorod arrays on different substrates](#)

Applied Physics Letters **96**, 263104 (2010); 10.1063/1.3442913

[TiO₂ based metal-semiconductor-metal ultraviolet photodetectors](#)

Applied Physics Letters **90**, 201118 (2007); 10.1063/1.2741128

[Low-temperature self-limiting atomic layer deposition of wurtzite InN on Si\(100\)](#)

AIP Advances **6**, 045203 (2016); 10.1063/1.4946786

[Photoconductivities in anatase TiO₂ nanorods](#)

Applied Physics Letters **105**, 153107 (2014); 10.1063/1.4898004

[Substrate impact on the low-temperature growth of GaN thin films by plasma-assisted atomic layer deposition](#)

Journal of Vacuum Science & Technology A: Vacuum, Surfaces, and Films **34**, 041511 (2016); 10.1116/1.4953463

[Low-temperature sequential pulsed chemical vapor deposition of ternary B_xGa_{1-x}N and B_xIn_{1-x}N thin film alloys](#)

Journal of Vacuum Science & Technology A: Vacuum, Surfaces, and Films **34**, 01A123 (2015); 10.1116/1.4936072



Instruments for Advanced Science

Contact Hiden Analytical for further details:

www.HidenAnalytical.com

info@hiden.co.uk

[CLICK TO VIEW](#) our product catalogue



Gas Analysis

- › dynamic measurement of reaction gas streams
- › catalysis and thermal analysis
- › molecular beam studies
- › dissolved species probes
- › fermentation, environmental and ecological studies



Surface Science

- › UHV TPD
- › SIMS
- › end point detection in ion beam etch
- › elemental imaging - surface mapping



Plasma Diagnostics

- › plasma source characterization
- › etch and deposition process reaction
- › kinetic studies
- › analysis of neutral and radical species



Vacuum Analysis

- › partial pressure measurement and control of process gases
- › reactive sputter process control
- › vacuum diagnostics
- › vacuum coating process monitoring

Enhanced photoresponse of conformal TiO₂/Ag nanorod array-based Schottky photodiodes fabricated via successive glancing angle and atomic layer deposition

Ali Haider

National Nanotechnology Research Center (UNAM), Bilkent University, Bilkent, Ankara 06800, Turkey
and Institute of Materials Science and Nanotechnology, Bilkent University, Bilkent, Ankara 06800, Turkey

Hilal Cansizoglu, Mehmet Fatih Cansizoglu, and Tansel Karabacak

Department of Physics and Astronomy, University of Arkansas at Little Rock, Little Rock, Arkansas 72204

Ali Kemal Okyay

National Nanotechnology Research Center (UNAM), Bilkent University, Bilkent, Ankara 06800, Turkey;
Institute of Materials Science and Nanotechnology, Bilkent University, Bilkent, Ankara 06800, Turkey; and
Department of Electrical and Electronics Engineering, Bilkent University, Bilkent, Ankara 06800, Turkey

Necmi Biyikli^{a)}

National Nanotechnology Research Center (UNAM), Bilkent University, Bilkent, Ankara 06800, Turkey
and Institute of Materials Science and Nanotechnology, Bilkent University, Bilkent, Ankara 06800, Turkey

(Received 26 August 2014; accepted 2 October 2014; published 20 October 2014)

In this study, the authors demonstrate a proof of concept nanostructured photodiode fabrication method via successive glancing angle deposition (GLAD) and atomic layer deposition (ALD). The fabricated metal-semiconductor nanorod (NR) arrays offer enhanced photoresponse compared to conventional planar thin-film counterparts. Silver (Ag) metallic NR arrays were deposited on Ag-film/Si templates by utilizing GLAD. Subsequently, titanium dioxide (TiO₂) was deposited conformally on Ag NRs via ALD. Scanning electron microscopy studies confirmed the successful formation of vertically aligned Ag NRs deposited via GLAD and conformal deposition of TiO₂ on Ag NRs via ALD. Following the growth of TiO₂ on Ag NRs, aluminum metallic top contacts were formed to complete the fabrication of NR-based Schottky photodiodes. Nanostructured devices exhibited a photo response enhancement factor of 1.49×10^2 under a reverse bias of 3 V. © 2014 American Vacuum Society. [<http://dx.doi.org/10.1116/1.4898203>]

I. INTRODUCTION

Recent progress in thin-film (TF) and nanostructured wide bandgap semiconductors have gathered significant interest toward their applications in ultraviolet (UV) photodetection.^{1,2} UV photodetectors have numerous applications in environmental monitoring, chemical and biological sensing, defense, and astronomy.³⁻⁵ Among the wide bandgap semiconductors, most influential widely used material families are SiC and III-nitrides.⁶⁻⁸ However, their practical applications in industry are hampered by their complex fabrication technology and high materials synthesis cost.^{9,10}

Having superior chemical, physical, and optical properties with wide bandgap, TiO₂ is regarded as a suitable candidate for utilization in UV photodetector fabrication technology.¹¹ Moreover, use of one-dimensional (1D) TiO₂ nanostructures can produce a remarkable improvement in device performance due to improved charge carrier collection and optical absorption. In the presence of metallic shell around the 1D nanostructures, contact area between semiconductor nanostructures and metal shell is significantly increased, which provide efficient carrier collection by introducing additional carrier transportation paths. Additionally, larger aspect ratio of 1D nanostructures also contribute toward efficient trapping of the incident radiation via diffuse light scattering and enhanced optical absorption.^{12,13}

Previously, TiO₂ 1D nanostructures fabricated by glancing-angle deposition (GLAD)^{12,13} and hydrothermal growth technique^{14,15} have been reported for the realization of highly sensitive Schottky type photodetectors. The observed enhanced photoresponsivity was attributed to the modification of oxygen species adsorbed at surface of TiO₂ nanorods (NRs) under illumination and trapped incident photons. However, in the case of metal-semiconductor nanostructures, effects of surface modification becomes irrelevant as metal covers all the concerned surface of semiconductor nanostructures.

Efficient charge carrier collection in photodetectors based on 1D semiconductor nanostructures is limited by random network nature and nonuniformity of nanostructured geometries.¹⁶ Uniform nanostructured geometries with larger aspect ratio can enhance the interface between metal and TiO₂ Schottky junction, which in turn decreases the transit time of generated carriers. Therefore, developing innovative, efficient, and cost-effective fabrication methods that can provide a variety of semiconductor nanostructures with uniform and optimized geometries for improving photodetector efficiencies might be of significant technological interest. For this reason, we propose to combine GLAD and atomic layer deposition (ALD) techniques in order to get metal-semiconductor geometry with a uniform and conformal interface with simple and cost-effective nanofabrication methods.

^{a)}Electronic mail: biyikli@unam.bilkent.edu.tr

GLAD, also called oblique angle deposition, is an alternative nanofabrication approach that offers the capability of producing well-aligned and well-separated nanostructures of a wide range of materials on almost any type of substrate.^{17–20} Enhanced light trapping in GLAD semiconductor NRs have already been studied and shown to be the main reason for superior optical absorption.^{13,17} Light trapping in GLAD metallic NRs will enhance the optical path in the semiconductor material embedded around NRs and subsequently results in high optical absorption in semiconductor material.²¹

ALD is a special version of chemical vapor deposition technique, in which the substrate is exposed to two alternating precursors in sequential steps separated by inert gas purges. Separate exposure of each precursor results in a monomolecular layer of exposed precursor which eventually becomes independent of the precursor exposure after consumption of all reactive surface sites. Due to self-limiting growth mechanism, ALD can serve to produce highly uniform and conformal coatings with precise thickness control on three-dimensional templates with high aspect ratios.²² In this study, we have fabricated a Schottky photodiode with ALD TiO₂ coated GLAD silver (Ag) NRs as a model material system to demonstrate the superiority of GLAD/ALD metal-semiconductor structures in the photodetection applications, which offers significantly enhanced photoresponse compared to conventional planar counterpart devices. Material and device characterization studies are carried out to reveal the structural, optical, and electrical properties of TiO₂ coated Ag NRs and detector performance of the fabricated nanostructured TiO₂-based Schottky photodiodes, respectively.

II. EXPERIMENT

A. ALD/GLAD TiO₂/Ag NRs-based photodiode fabrication

Photodiode device fabrication based on successive combination of GLAD and ALD to produce metal-semiconductor NR arrays is carried out in the following three steps:

- (1) Sputtering of Ag TF on Si substrate followed by GLAD of Ag NRs.
- (2) TiO₂ deposition on Ag NRs via thermal ALD using exposure mode.
- (3) Aluminum (Al) metallic top contact deposition on TiO₂ coatings by thermal evaporation using shadow mask.

Details of the fabrication process are given in Subsections II A 1–II A 3.

1. Sputtering of Ag TF and GLAD Ag NRs

Ag TF and NRs were deposited on Si substrate (University Wafers, p-type, (100), 1–10 Ω cm) in a custom designed sputtering GLAD system. 99.99% purity Ag target (from Kurt Lesker) was used as the source material. The TF and GLAD NRs depositions were carried out at room temperature under $\sim 3 \times 10^{-6}$ mbar base pressure and at 1.5×10^{-3} mbar working gas (Ar) pressure. An Ag film was deposited underneath Ag NRs and GLAD was utilized to

form Ag NRs.^{19,20} The substrate was positioned at an 85° incidence angle measured between the incident flux and the substrate normal. During GLAD, incident flux reaches substrate at a high angle and is dominantly captured by taller features, which shadow the shorter features on the substrate. This so called “shadowing effect” results in isolated structures, which are bent toward incident flux direction. A sufficient substrate rotation around the substrate normal axis can help the isolated structures grow in the vertical direction instead of flux direction and results in isolated vertical NRs (details of GLAD can be found elsewhere).¹³ In this study, a continuous substrate rotation at 5 rpm (rotation per minute) was used during NRs depositions. The same substrate rotation was used for also TF in order to get a uniform film on the substrate.

2. ALD of TiO₂ on Ag NRs

Ag NRs grown on Ag TF/Si were introduced into the ALD system (Savannah S100 ALD reactor, Cambridge Nanotech Inc.) and coated with TiO₂. TiO₂ layer growth was performed at 150 °C by ALD using tetrakis(dimethylamino)titanium [Ti(NMe₂)₄], and water (H₂O) as titanium and oxygen precursors, respectively. Ti(NMe₂)₄ was preheated to 75 °C and stabilized at this temperature prior to growth experiment. Preheating was necessary to increase the vapor pressure of the precursor which in turn increases the growth per cycle of TiO₂. Growth of TiO₂ was carried out in exposure mode of ALD using 1000 growth cycles, in which dynamic vacuum was switched to static vacuum just before the metal precursor and oxidant pulses, and switched back to dynamic vacuum before the purging periods after waiting for some time, which is called exposure time (a trademark of Cambridge Nanotech Inc.). For nanostructures of high aspect ratio, the extra exposure time is necessary to allow precursor vapors to diffuse into the nanostructures in order to provide highly conformal growth of desired material.²³ Flow rate of N₂ is normally 20 standard cubic centimeters per minute (SCCM), which was set to 10 SCCM just before dynamic vacuum was switched to static vacuum. Precursor pulse lengths of 0.1 and 0.015 s were used for Ti(NMe₂)₄ and (H₂O), respectively. Each precursor was exposed to the substrate for an exposure time of 10 s which was followed by purge period of 20 s. In the same run, TiO₂ was deposited on Ag-TF/Si to fabricate Ag/TiO₂ planar counterpart of GLAD/ALD based Ag/TiO₂ nanostructured device. Moreover, in the same run, TiO₂ was also deposited on planar Si (100) and double side polished quartz wafers in order to measure the thickness of deposited TiO₂ and transmission spectra of deposited TiO₂ TFs, respectively. The thickness of the deposited TiO₂ on Si was measured by using a variable angle spectroscopic ellipsometer (J. A. Woollam). Ellipsometric spectra of the sample that was recorded in the wavelength range of 300–1000 nm at three angles of incidence (65°, 70°, and 75°) were fitted by using a Cauchy dispersion model. The thickness of the TiO₂ film was measured as ~ 50 nm, which corresponds to a growth rate of 0.50 Å/cycle. The recipe optimization is given elsewhere.²³

3. Aluminum (Al) metallic top contact deposition

As a last step, Al metallic top contacts were deposited on Ag/TiO₂ NR and Ag/TiO₂ TF samples via thermal evaporation using patterned 2 × 2 cm² copper shadow masks with 1 mm diameter circular apertures. Al pellets (Kurt J. Lesker, 99.99% pure) were used to evaporate Al in thermal evaporator (Vaksis, PVD vapor-3 s Thermal) with base pressure of 6.6 × 10⁻⁶ Torr.

B. Material characterization

Surface morphology, film thickness, and NRs length were measured using scanning electron microscopy (SEM) [JEOL 7000F SEM and Quanta 200 FEG SEM (FEI)]. Spectral transmission measurements were performed with a UV-VIS spectrophotometer [Ocean Optics HR4000CG-UV-near infrared (NIR)] in the wavelength range of 220–1000 nm relative to air. The total reflection (including diffuse reflection) in GLAD Ag nanorods was measured with Shimadzu UV-3600 spectrophotometer incorporated with an integrating sphere (ISR-3100 Integrating Sphere Attachment) in the wavelength range of 300–1600 nm. Dark and illuminated current–voltage (I–V) measurements were performed using semiconductor parameter analyzer (Keithley, 4200–SCS).

The photodetector relative responsivity, defined as I_{on}/I_{off} , where I_{on} and I_{off} are the illuminated and the dark currents, respectively, and photoresponse (A/W), defined as I_{on}/Θ , where Θ represents the optical power per unit area illuminating the sensitive region on the sample, were both measured at different wavelengths of laser diodes. Four different laser diodes with emission wavelengths of 405, 532, 635, and 780 nm were used to measure the spectral dependence of the device photoresponses.

III. RESULTS AND DISCUSSION

Figures 1(a) and 1(b) show the SEM images of cross sectional and top view of Ag TF deposited by sputtering on Si substrate, respectively. Average thickness of the film was

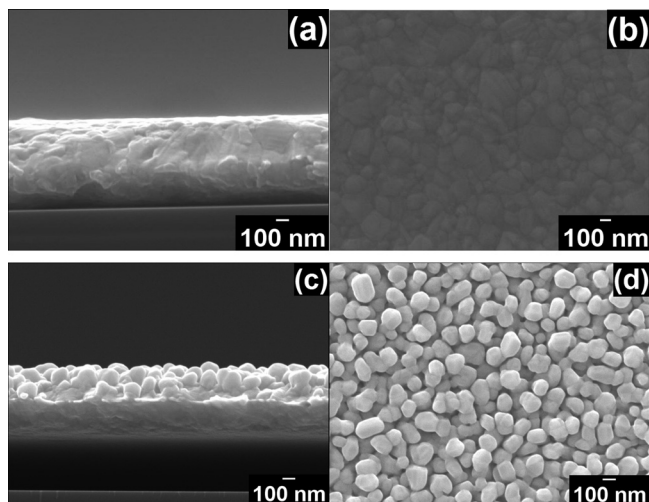


FIG. 1. (a) Cross sectional and (b) top view SEM images of Ag TF deposited on Si by sputtering, respectively. (c) and (d) Cross sectional and top view SEM images of Ag NRs deposited on Ag TF/Si by GLAD, respectively.

measured as 350 nm through SEM image analysis. Figures 1(c) and 1(d) show the SEM images of Ag NRs deposited by GLAD on Ag TF coated Si substrate. Figure 1(c) shows the cross-sectional view of Ag NRs, which depicts the perpendicular columnar structure of Ag NRs. The length and diameter of Ag NRs varies between ~120–200 nm and ~100–130 nm, respectively. Figure 1(d) shows the top view of Ag NRs, which reveals the homogeneous distribution of Ag NRs over the substrate surface. Through SEM images, the NRs were observed to be isolated enough to deposit TiO₂ coating and also enhance the light trapping, which potentially increase the optical absorption and thus the photoresponse of TiO₂ coating.

Following the fabrication of Ag NRs by GLAD, TiO₂ was deposited using exposure-mode ALD. The amorphous as-deposited TiO₂ was converted to anatase phase of TiO₂ after annealing in air ambient at 450 °C for 1 h.²³ SEM images of the annealed TiO₂ deposited on Ag NRs are shown in Figs. 2(a) and 2(b), which represents the tilted and top view of Ag/TiO₂ NRs, respectively. These SEM images reveal the conformal and uniform coating of TiO₂ on Ag NRs by virtue of self-limiting reactions of ALD.

Normal incidence transmission spectra of annealed TiO₂ TF samples deposited on double side polished quartz substrates in the UV-VIS and Near infrared (NIR) regions

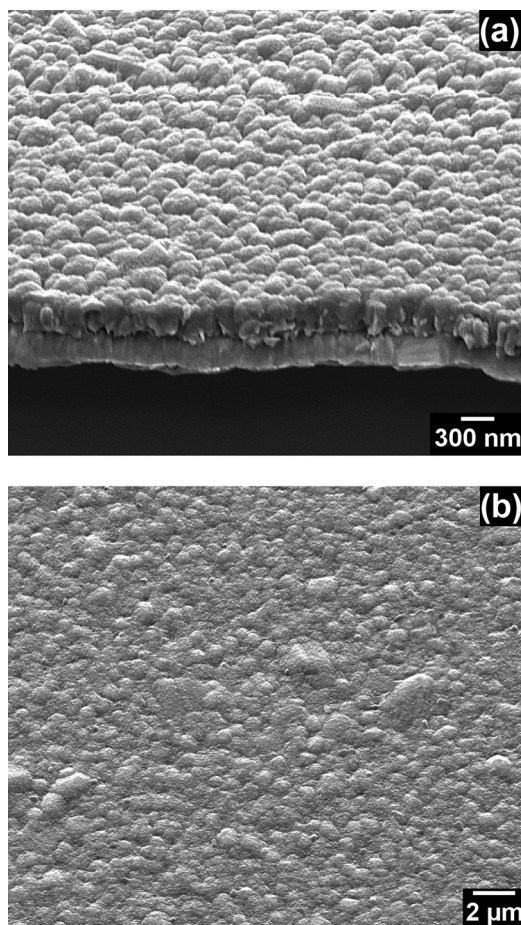


FIG. 2. (a) Tilted and (b) top view SEM images of TiO₂ deposited on Ag NRs/Ag TF/Si by ALD, respectively.

are presented in Fig. 3(a). Significant absorption was observed at UV wavelengths less than 350 nm, which is believed to be originated due to main band-to-band absorption. In the visible and near infrared regime, the transmission increases gradually without clear saturation till 1000 nm. The impurity content and defect centers in the film may give rise to absorption and scattering centers, which might be the possible cause of optical loss in visible and near infrared regimes.²⁴ Total reflection (combination of diffuse and specular reflection) spectra of Ag TF and NRs deposited on Si substrates in the UV-VIS and NIR regions are presented in Fig. 3(b). The average reflection of Ag TF was measured to be in the 90%–95% range within the visible and infrared spectrum which shows highly reflecting nature of Ag TF. Significant decrease in reflection was observed at UV wavelengths less than 320 nm, which is the onset of interband absorption related with either transition from Fermi surface to upper next unfilled band or from lower lying filled band to Fermi surface. Ag NRs show considerably less reflectance as compared to Ag TF, which is believed to be due to surface plasmon resonance of Ag NRs.^{25,26}

Figure 4 represents the schematic of the fabricated NRs-based and corresponding TF device while the inset shows

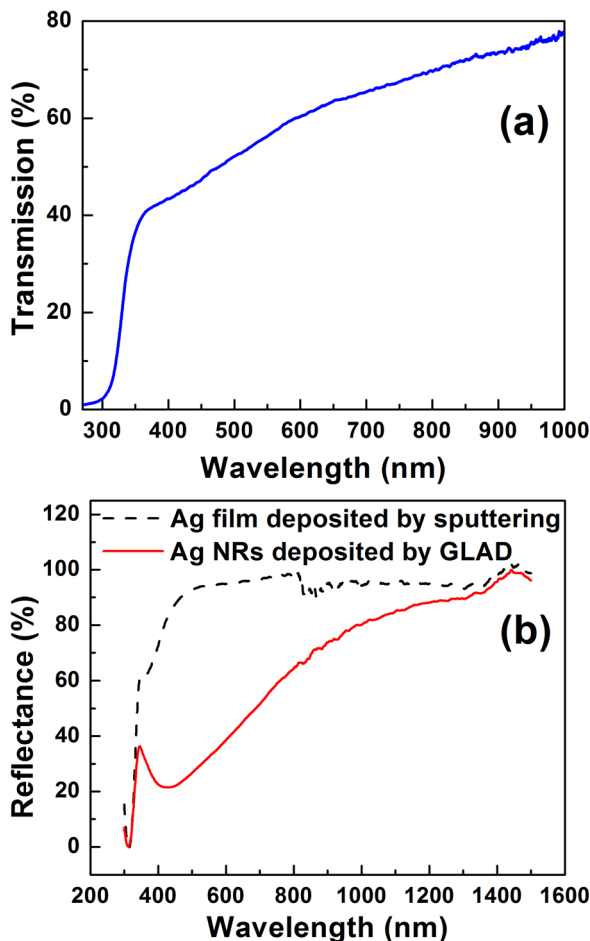


Fig. 3. (Color online) (a) Optical transmission spectrum of the ~50 nm thick TiO₂ thin-film deposited on double side polished quartz wafer. (b) Total reflection (combination of diffuse and specular reflection) spectra of Ag TF and NRs deposited on Si substrates in the UV-VIS and NIR regions.

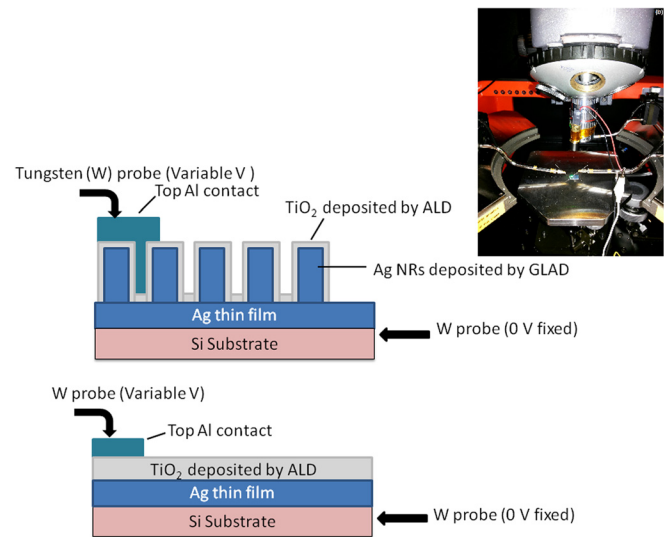


Fig. 4. (Color online) Schematic of the fabricated NRs-based and corresponding TF device (top to bottom, respectively) and (inset) semiconductor parameter analyzer utilized for measuring dark and illuminated I–V characteristics of the devices.

the bias-dependent dark current and illuminated photocurrent measurement setup. Variable bias voltage was applied to top Al contact where as highly doped Si substrate was the bottom contact, which was kept grounded at 0 V. Figures 5(a)

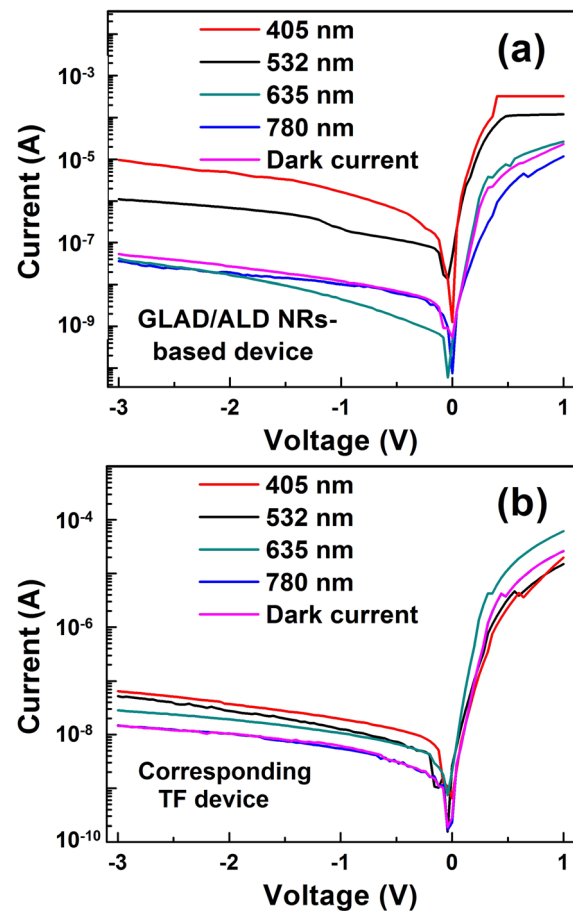


Fig. 5. (Color online) Current–voltage characteristics of the fabricated (a) Al/TiO₂/Ag(NRs)/Ag(TF)/Si and (b) Al/TiO₂/Ag(TF)/Si photodiode samples under illuminated and dark conditions.

and 5(b) shows the I–V characteristics of the fabricated Al/TiO₂/Ag(NRs)/Ag(TF)/Si and reference Al/TiO₂/Ag(TF)/Si photodiode samples in dark and under illumination with different laser sources, respectively. It can be seen that both devices exhibit rectification under either dark or laser-illuminated conditions, indicating the successful formation of a Schottky junction between Al and TiO₂. The measured reverse (I_R) and forward (I_F) currents at 1 V in dark were found to be 1.2×10^{-8} and 2.3×10^{-5} A, respectively, for GLAD/ALD NR-based device and the corresponding rectification ratio I_F/I_R is $\sim 1.9 \times 10^3$. A significant increase in reverse current (photocurrent) of NRs-based photodiode is observed upon illumination with laser diodes at 3 V. The increase in reverse current is more prominent in both NRs-based device and TF counterpart as laser-diode wavelengths approach UV spectrum. As the energy of photon gets closer to the bandgap of anatase TiO₂ (~ 3.2 eV), more and more electron-hole pairs are generated, which contribute to the cumulative photocurrent.²⁷ Photocurrent of NR-based device at reverse bias of 3 V is considerably higher than their TF-based counterparts. Reverse current in both the NRs-based device and TF counterpart tends to become constant below the reverse bias of 1.5 V, which might be due to total depletion of TiO₂ layer.

Relative responsivity of the GLAD/ALD NRs-based device and corresponding TF device is presented in Figs. 6(a) and 6(b), respectively. The relative responsivity of GLAD/ALD NRs-based device at reverse bias of 3 V was measured as 1.81×10^2 , while relative responsivity of corresponding TF device at reverse bias of 3 V was 4.8 for illumination with 405 nm wavelength laser diode. The relative responsivity values at 635 and 732 nm were very low and indistinguishable for GLAD/ALD NRs-based device while the relative responsivity value at 532 nm was measured as 20.7 and 3.6 for GLAD/ALD NRs-based device and corresponding TF device, respectively. The relative responsivity is almost constant within the reverse biasing range from 1.5 to 3 V in GLAD/ALD NRs-based device. Constant relative responsivity within the reverse biasing range from 1.5 to 3 V might be attributed to total depletion of TiO₂ layer and the similar difference of current value between the dark and illuminated current along the biasing range. Figure 7 reveals the photoresponse of both NRs and corresponding TF photodiode device, operating at the reverse bias voltage of 3 V. The photoresponse of NR-based device to radiation wavelength of 405 nm sharply increases in comparison with the corresponding TF device. Photoresponse enhancement factor (ratio of photoresponse of NRs-based device to corresponding TF device) of 1.49×10^2 was achieved at 405 nm.

The enhanced device photoresponse might be attributed to the increase in optical absorption and efficient carrier transportation and collection in metal-semiconductor NR array geometry. The perpendicular NR array can trap the incident photons due to improved scattering of light inside the NR structure. Enhanced scattering of incident photons increased the optical absorption, which leads to improve electron-hole pair generation process.^{12,13} Higher number of charge carriers can be generated in NRs-based device

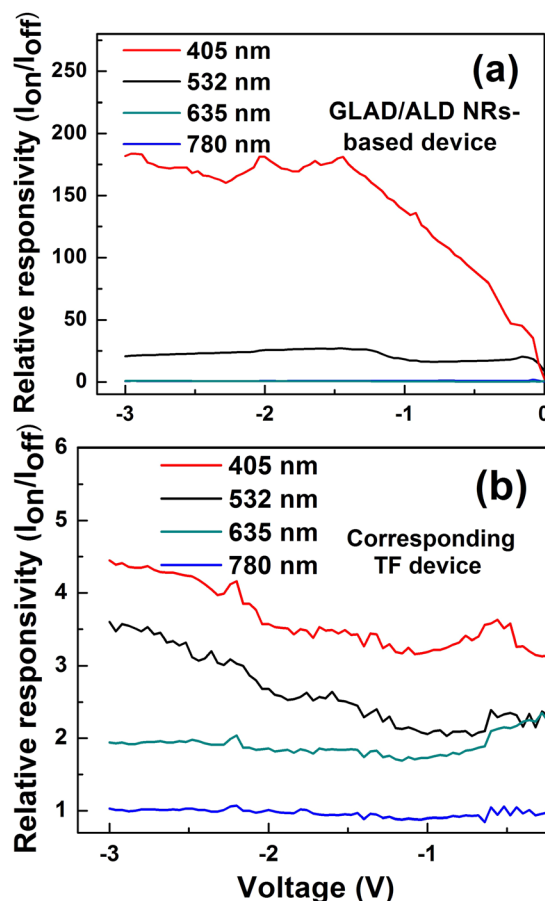


Fig. 6. (Color online) Relative responsivity values measured vs applied reverse bias of the fabricated (a) Al/TiO₂/Ag(NRs)/Ag(TF)/Si and (b) Al/TiO₂/Ag(TF)/Si photodiodes under illumination of different laser diodes.

compared to TF counterpart whose optical absorption is relatively low. Additionally, metal-semiconductor NR array geometry can introduce a radial junction at the metal semiconductor interface whereas a planar junction is formed at the TF device. High aspect ratio of GLAD NRs and

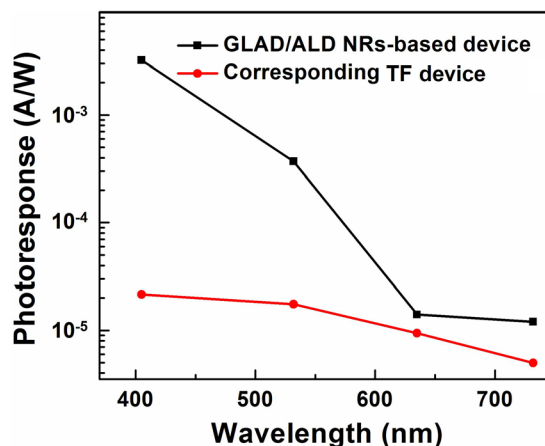


Fig. 7. (Color online) Photoresponse measured from the fabricated Al/TiO₂/Ag(NRs)/Ag(TF)/Si and Al/TiO₂/Ag(TF)/Si under illumination from laser diodes of different wavelengths measured at reverse bias of 3 V, respectively.

fairly uniform and conformal ALD coating can enhance the interface area of the junction in NRs-based device, which help more carriers be collected compared to the TF device.

IV. SUMMARY AND CONCLUSIONS

We have demonstrated a photodiode fabrication method, which combines GLAD and ALD to fabricate Ag/TiO₂ NR arrays, which exhibit enhanced photoresponse performance in comparison with their conventional TF counterparts. Measurements and analysis have revealed that the device shows a photoresponse enhancement factor of 1.49×10^2 . A significant improvement in relative responsivity and photoresponse was observed over the Ag/TiO₂ corresponding TF photodetector, which was attributed to improved charge collection and transportation in NRs-based device due to higher interface of metal-semiconductor junction and trapped incident photons due to enhanced optical path of radiations. Aspect ratio of NRs and thickness of ALD deposited semiconductor material needs to be optimized in order to further improve the device efficiency. The successive GLAD and ALD technique can be applied to other metal/semiconductor material combinations as well to enhance photodetector device performance.

ACKNOWLEDGMENTS

This collaborative work was performed at Bilkent University—National Nanotechnology Research Center (UNAM) supported by the Ministry of Development of Turkey through the National Nanotechnology Research Center Project and at University of Arkansas at Little Rock (UALR) with the support of National Science Foundation (NSF, Grant Nos.: EPS-1003970 and 1159830). This work was supported in part by the Scientific and Technological Research Council of Turkey (TUBITAK) with Grant Nos. 109E044, 112M004, 112E052, 112M578, and 113M815. N.B. and A.K.O. acknowledge support from FP-7 Marie Curie International Re-integration Grant (Grant No. PIRG05-GA-2009-249196 and PIRG04-GA-2008-239444, respectively). A.H. acknowledges Higher Education Commission of Pakistan (HEC) for Human Resource Development (HRD) fellowship for MS leading to Ph.D. The authors also thank the staff of UALR Center for

Integrative Nanotechnology Sciences for their support in SEM and UV-VIS spectrometer measurements.

- ¹S. J. Young, L. W. Ji, S. J. Chang, and Y. K. Su, *J. Cryst. Growth* **293**, 43 (2006).
- ²S. J. Young, L. W. Ji, T. H. Fang, S. J. Chang, Y. K. Su, and X. L. Du, *Acta Mater.* **55**, 329 (2007).
- ³M. Razeghi and A. Rogalski, *J. Appl. Phys.* **79**, 7433 (1996).
- ⁴E. Monroy, F. Calle, J. L. Pau, E. Munoz, F. Omnes, B. Beaumont, and P. Gibart, *J. Cryst. Growth* **230**, 537 (2001).
- ⁵E. Ozbay, N. Biyikli, I. Kimukin, I. Kimukin, T. Tut, T. Kartaloglu, and O. Aytur, *IEEE J. Sel. Top. Quantum Electron.* **10**, 742 (2004).
- ⁶C. J. Collins, U. Chowdhury, M. M. Wong, B. Yang, A. L. Beck, R. D. Dupuis, and J. C. Campbell, *Appl. Phys. Lett.* **80**, 3754 (2002).
- ⁷Y. Z. Chiou and J. J. Tang, *Jpn. J. Appl. Phys., Part 1* **43**, 4146 (2004).
- ⁸M. Mazzillo, G. Condorelli, M. E. Castagna, G. Catania, A. Sciuto, F. Roccaforte, and V. Raineri, *IEEE Photonics Technol. Lett.* **21**, 1782 (2009).
- ⁹S. J. Pearton, F. Ren, A. P. Zhang, and K. P. Lee, *Mater. Sci. Eng., R* **30**, 55 (2000).
- ¹⁰Y. Han, G. Wu, M. Wang, and H. Chen, *Appl. Surf. Sci.* **256**, 1530 (2009).
- ¹¹M. Zhang, H. F. Zhang, K. B. Lv, W. Y. Chen, J. R. Zhou, L. Shen, and S. P. Ruan, *Opt. Express* **20**, 5936 (2012).
- ¹²P. Chinnamuthu, J. C. Dhar, A. Mondal, A. Bhattacharyya, and N. K. Singh, *J. Phys. D: Appl. Phys.* **45**, 135102 (2012).
- ¹³H. Cansizoglu, M. F. Cansizoglu, M. Finckenor, and T. Karabacak, *Adv. Opt. Mater.* **1**, 158 (2013).
- ¹⁴H. Karaagac, L. E. Aygun, M. Parlak, M. Ghaffari, N. Biyikli, and A. K. Okyay, *Phys. Status Solidi RRL* **6**, 442 (2012).
- ¹⁵H. Zhang, S. p. Ruan, H. Li, M. Zhang, K. Lv, C. Feng, and W. Chen, *IEEE Electron Device Lett.* **33**, 83 (2012).
- ¹⁶X. Wang, W. Tian, M. Liao, Y. Bando, and D. Golberg, *Chem. Soc. Rev.* **43**, 1400 (2014).
- ¹⁷M. F. Cansizoglu, R. Engelken, H. W. Seo, and T. Karabacak, *ACS Nano* **4**, 733 (2010).
- ¹⁸N. O. Young and J. Kowal, *Nature* **183**, 104 (1959).
- ¹⁹K. Robbie, M. J. Brett, and A. Lakhtakia, *Nature* **384**, 616 (1996).
- ²⁰T. Karabacak and T.-M. Lu, "Shadowing growth and physical self-assembly of 3D columnar structures," *Handbook of Theoretical and Computational Nanotechnology*, edited by M. Rieth and W. Schommers (American Scientific, Stevenson Ranch, CA, 2005), p. 729.
- ²¹R. B. Abdulrahman, A. S. Alagoz, and T. Karabacak, "Enhanced light trapping in periodic aluminum nanorod arrays as cavity resonator," *MRS Proceedings* (Cambridge University, 2013), Vol. 1566.
- ²²C. Ozgit-Akgun, F. Kayaci, I. Donmez, T. Uyar, and N. Biyikli, *J. Am. Ceram. Soc.* **96**, 916 (2013).
- ²³H. Ceylan, C. Ozgit-Akgun, T. S. Erkal, I. Donmez, R. Garifullin, A. B. Tekinay, H. Usta, N. Biyikli, and M. O. Guler, *Sci. Rep.* **3**, 2306 (2013).
- ²⁴L. Bedikyan, S. Zakhariyev, and M. Zakhariyeva, *J. Chem. Technol. Metall.* **48**, 555 (2013), available at http://dl.uctm.edu/journal/node/j2013-6/2-Bedikyan_p-555-558.pdf.
- ²⁵Y. Lu, H. Zhang, and F. Liu, *Phys. Lett. A* **342**, 351 (2005).
- ²⁶A. Tao, F. Kim, C. Hess, J. Goldberger, R. He, Y. Sun, Y. Xia, and P. Yang, *Nano Lett.* **3**, 1229 (2003).
- ²⁷F. Hossein-Babaei, M. M. Lajvardi, and F. A. Boroumand, *Sens. Actuators, A* **173**, 116 (2012).